Journal of Ceramic Processing Research. Vol. 16, No. 2, pp. 276~279 (2015)

J O U R N A L O F
Ceramic Processing Research

Electrical characteristics of $InZnO_3$ transistors fabricated by reverse offset printing

Yong Suk Yang[a,]*, Ju-hyeon Park[b], In-Kyu You[a], Sung-Hoon Hong[a], Ho-Gyeong Yun[a], Young Hun Kang[c], Changjin Lee[c] and Song Yun Cho[c]

[a]*Electronics and Telecommunications Research Institute (ETRI), 138 Gajeong, Yuseong, Daejeon 305-700, Korea*
[b]*Poongsan, 2222-2 Sandae, Ankang, Kyeongju, Kyeongsangbukdo, 780-801, Korea*
[c]*Korea Research Institute of Chemical Technology (KRICT), 141 Gajeong, Yuseong, Daejeon 305-600, Korea*

The emerging technology of printed electronics will replace traditional photolithography, which requires costly materials, complex processes and expensive equipment, for the production of electronic circuits and displays. In this study, we fabricated thin-film transistors (TFTs) based on the materials of indium zinc oxide (IZO) semiconductor and Ag metal. The source-drain electrodes were fabricated on IZO film by a reverse offset printing method and annealed at various temperatures. The performance of the IZO TFTs with regard to the annealing temperature was investigated by examining the *I-V* characteristics. The electrical mobility of the TFTs increased as the annealing temperature increased. Inter-diffusion between the printed Ag metal and the IZO semiconductor was observed in the depth concentration profile of the Ag/IZO/SiO_2/Si sample annealed at 250 °C.

Key words : Reverse offset printing, indium zinc oxide, Thin film transistors, Electrical mobility, Depth concentration profile.

Introduction

The intrinsic properties of oxide semiconductors, such as their high mobility and low leakage current, have been very important in the area of liquid crystal displays (LCDs) and organic light-emitting displays [1-4]. In addition, solution-processable devices and manufacturing techniques of thin-film transistors (TFTs) using these materials have also been studied in an effort to derive low-cost and low-temperature manufacturing processes [5-7]. However, it is not possible to fabricate high-performance TFTs at lower temperatures by solution processes such as printing. A recent development direction for TFTs created by a solution process is to ensure that the ink materials of the semiconductor and the metal-semiconductor junction have a low work function [8, 9].

In this study, indium zinc oxide ($InZnO_3$, IZO) semiconductor TFTs were prepared using the solution processes of spin-coating and a reverse offset printing (ROP). To make source-drain electrodes in the TFTs, Ag was printed on IZO/SiO_2/Si substrates by means of a roll plate-to-plate ROP method. The surface and cross-sectional morphologies of the printed Ag films were observed using a scanning electron microscope (SEM). The electrical properties of IZO TFTs created with various annealing conditions were investigated by examining their current-voltage characteristics.

*Corresponding author:
Tel : +82-42-860-1171
Fax: +82-42-860-6495
E-mail: jullios@etri.re.kr

Experimental

The IZO thin films were fabricated on SiO_2(300 nm)/Si substrates by a spin-coating method. Zinc acetylacetonate hydrate ($Zn(C_5H_7O_2)_2xH_2O$) and indium nitrate hydrate ($In(NO_3)_3xH_2O$) (all from Sigma-Aldrich) were employed for the preparation of the IZO precursor solutions. The total concentration of the IZO precursor was fixed at 0.1 M and the molar ratio of indium nitrate hydrate to zinc acetylacetonate hydrate was 1 : 1. The SiO_2(300 nm)/Si substrates, which were heavily p-type doped and thermally oxidized silicon wafers, were prepared as substrates after cleaning them sequentially with acetone and isopropyl alcohol for 10 min during each step and then rinsing them with deionized water. The IZO solution was then filtered using a 0.1-μm syringe filter and spin-coated at 4000 rpm onto the substrates. The IZO/SiO_2/Si samples were annealed on a hot plate at 300 for 2 h.

Ag as a source-drain electrode was printed on the IZO/SiO_2/Si samples using a roll plate-to-plate ROP method (Narae Nanotech Co.), as illustrated in Fig. 1(a). The Ag paste ink was made of Ag nanoparticles (Advanced Nano Products Co.). The Ag content and viscosity of the ink were approximately 39 wt% and 1.5 cps, respectively. The Ag ink was manipulated by a syringe pump and dispensed onto the surface of a poly-dimethylsiloxane blanket roll (KNW Co.). A glass cliché with the source-drain electrode patterns was prepared through a wet-etching process using a Cr metal mask and hydrogen fluoride. As the blanket was rolled over the cliché with intaglio patterns, unnecessary

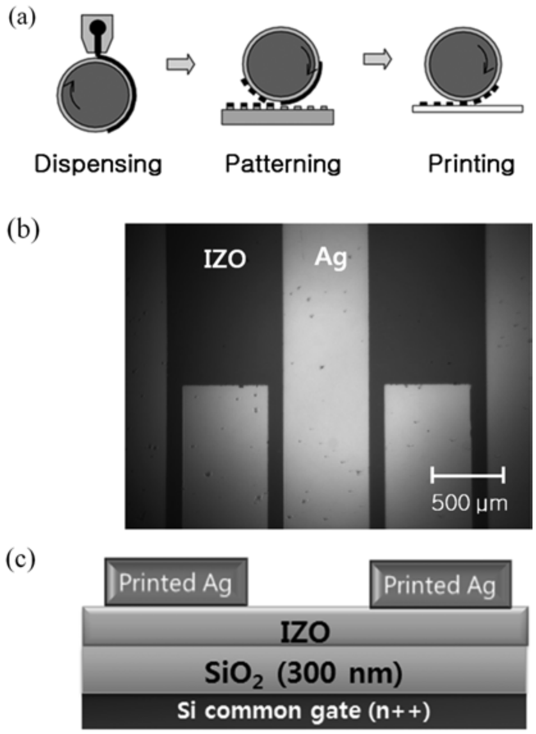

Fig. 1. (a) Schematic diagram of ROP process, (b) optical image of the source-drain Ag electrodes fabricated by ROP, and (c) schematic picture of IZO TFTs.

ink was removed from the blanket and was transferred onto the top surface of the cliché. The remaining Ag ink, which was in the desired pattern on the blanket, was transferred onto the $IZO/SiO_2/Si$ samples.

After the ROP process, the samples were annealed at temperatures ranging from 120 °C and 250 °C for 30 min. Figure 1(b) shows an image of a printed source-drain electrode taken with an optical microscope. The annealing condition of the sample was at 250 °C for 30 min. The printed Ag in the IZO films resembled the designed pattern in terms of its shape. The length and width of the channel of the sample were 100 and 10000 μm, respectively. The structure of the IZO TFTs is shown in Fig. 1(c). To compare the characteristics of the IZO TFTs, Al as a source-drain electrode was deposited in situ on $IZO/SiO_2/Si$ using a conventional thermal evaporator at a pressure of below 10^{-4} Pa. The electrical properties of the IZO TFTs and the depth concentration profile of the $Ag/IZO/SiO_2/Si$ samples were measured using a semiconductor characterization system (Keithley 4200) and an Auger electron spectroscope (AES), respectively.

Results and Discussion

Figures 2(a), 2(b), 2(c), and 2(d) show cross-sectional SEM images of $Ag/IZO/SiO_2/Si$ samples annealed at 120, 150, 220, and 250 °C for 30 min, respectively. As the annealing temperature increased, the thickness of the Ag films in the SEM image decreased. In Figs. 2(a)-2(d), the measured values of

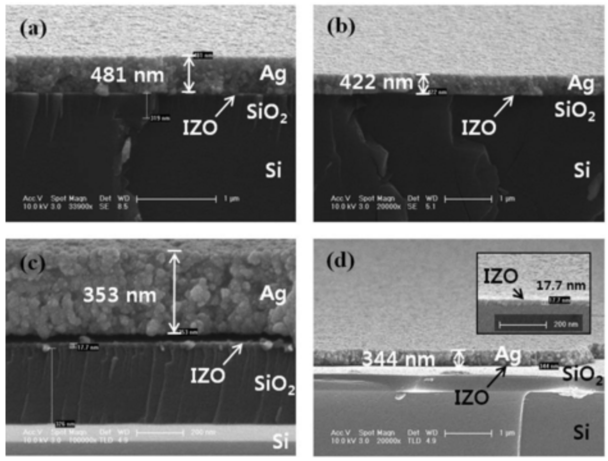

Fig. 2. SEM images of $Ag/IZO/SiO_2/Si$ samples annealed at (a) 120, (b) 150, (c) 220, and (d) 250 °C for 30 min. The inset of Fig. 2(d) is the SEM image of $IZO/SiO_2/Si$ sample.

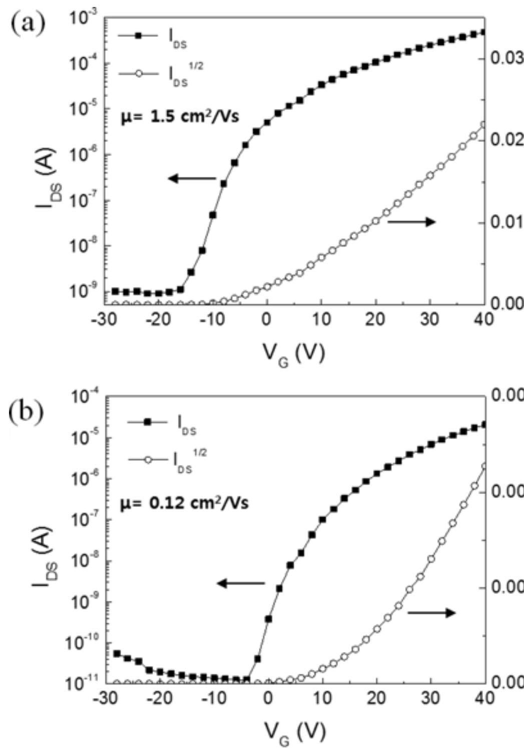

Fig. 3. Transfer characteristics of the IZO TFTs with the source-drain electrodes of (a) evaporated Al and (b) ROP Ag.

the Ag thickness are shown to be approximately 481, 422, 353, and 344 nm, respectively. This is related to the grain growth and the densification of the Ag nanoparticles, which were fortified with an increase in the annealing temperature. In Fig. 2(c), the average value of the grain size in the Ag film is approximately 87 nm. The thickness of the IZO film shown in the inset of Fig. 2(d) is approximately 17.7 nm, as measured in the sample with the $IZO/SiO_2/Si$ structure.

Figures 3(a) and 3(b) illustrate the transfer characteristics of the saturation region ($V_{DS} = 40$ V) for IZO TFTs with various source-drain materials. The metals of the source-

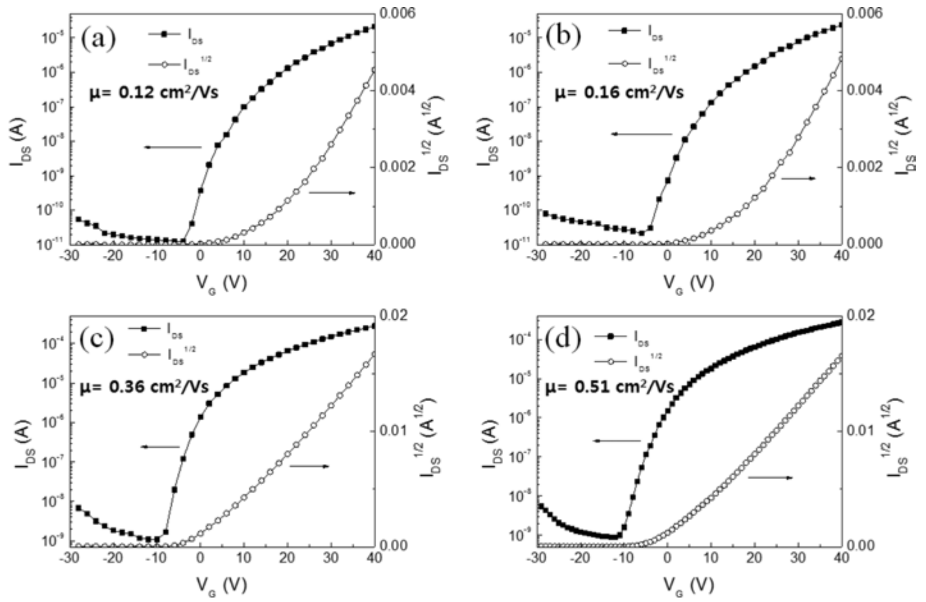

Fig. 4. Transfer characteristics of the ROP Ag/IZO TFTs annealed at (a) 120, (b) 150, (c) 220, and (d) 250 ºC for 30 min.

drain electrode used were evaporated Al (Fig. 4(a)) and ROP Ag (Fig. 4(b)). In all of the evaporated Al and ROP Ag samples, the lengths and widths of channel were 100 μm and 10000 μm, respectively. The annealing condition in the Ag/IZO/SiO_2/Si TFTs was at 120 ºC for 30 min, respectively. We extracted the field effect mobility (μ) and threshold voltage (V_{th}) based on the standard MOSFET equation [10].

The μ and V_{th} values in the IZO TFTs with the evaporated Al electrodes were determined to be approximately 1.5 cm^2/Vs and −17 V, respectively. In addition, the μ and V_{th} values for the ROP Ag electrodes were approximately 0.12 cm^2/Vs and –4.4 V, respectively. We surmised that the difference in the transfer characteristics of the IZO TFTs fabricated on different electrodes can be attributed to the characteristics of the charge carrier injection between the semiconductor and the metal electrode. The value of the bulk band gap of IZO was determined to be approximately 3 eV, and the IZO material pins slightly above the charge neutrality level, resulting in a negative surface charge from the occupied acceptor surface states and upward bending of the bands relative to the Fermi level, according to a previous study [11]. ROP Ag metal is generally known to have a work function larger than that of Al [12]. The larger work function of the ROP Ag is expected to obstruct the electron injection from the metal electrode to the semiconductor even further.

Figures 4(a), 4(b), 4(c), and 4(d) represent the transfer characteristics of the saturation region (V_{DS} = 40 V) of the ROP Ag/IZO TFTs annealed at 120, 150, 220, and 250 ºC for 30 min, respectively. The mobility of the IZO TFTs annealed at 120 ºC was relatively low and it increased as the annealing temperature increased. In Figs. 4(a)-4(d), the obtained mobility levels of the IZO TFTs are approximately 0.12, 0.16, 0.36, and 0.51 cm^2/Vs, respectively. On the other hand, the V_{th} values of the IZO TFTs shifted toward the negative voltage direction as the annealing temperature increased. As shown in Fig. 4(d), the V_{th} value of the IZO TFT

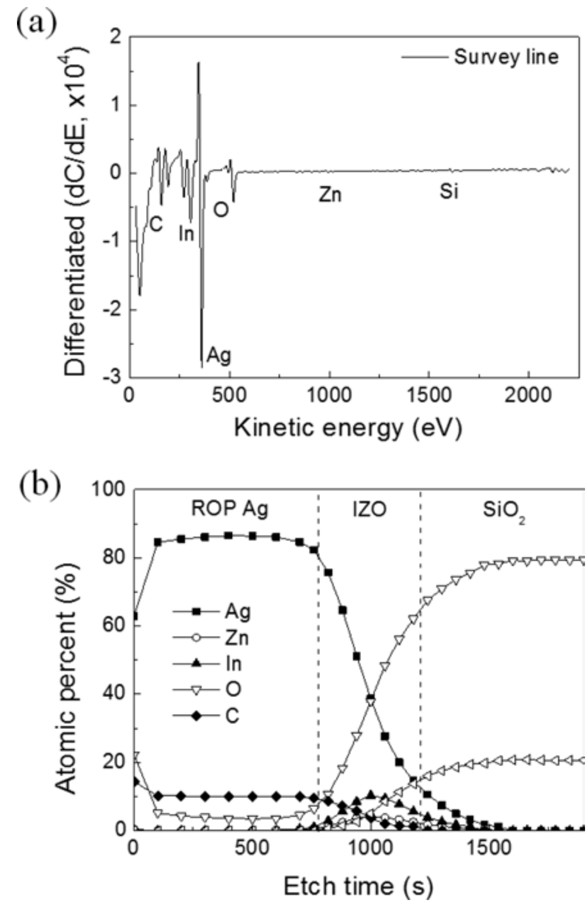

Fig. 5. (a) AES survey and (b) depth concentration profile of elements on the Ag/IZO/SiO_2/Si sample. The sample annealed at 250 ºC for 30 min.

annealed at 250 °C was approximately −12.1 V.

To understand these results, we investigated the depth concentration profiles of elements from AES surveys with regard to $Ag/IZO/SiO_2/Si$ samples etched for various etching times, indicative of the depths from the surface. The annealing condition of the sample was 250 °C for 30 min. Because the thickness of the Ag was much greater than that of the IZO, a pre-etching step was done to remove the upper part of the printed Ag layer before the AES measurements. The Auger spectra were obtained for the kinetic energies of the electrons within the range of 0 to 2000 eV for the main elements in the samples. The results of samples obtained after ion etching for certain depths are presented in Fig. 5(a). Etching was done with argon ions having an energy level of 3 keV, and the diameter of the beam was 1 mm. The etching depth was calculated on the assumption of an etching rate of 3 Å/min. The surface cleaning quality was estimated using the Auger peaks of carbon. Figure 5(b) shows the distribution profiles of the relative element concentrations in the $Ag/IZO/SiO_2/Si$ sample. Inter-diffusion between the printed Ag metal and the IZO semiconductor was observed in the depth concentration profile of the sample. The diffusion of the Ag element into IZO film with an increase in the annealing temperature was studied by Kim [13]. They reported that the interface layer became thicker and the contact between the Ag and the IZO became ohmic as the annealing temperature was increased [13]. We deduced that the ohmic contact was mainly the cause of the decrease of the electrical barrier between the Ag and IZO, leading to the improvement of the electric properties via the increase in the electron injection.

Summary

In this study, we fabricated IZO TFTs by spin-coating and ROP processes and investigated their electric characteristics under various annealing conditions. The μ and V_{th} values in the ROP $Ag/IZO/SiO_2/Si$ TFTs annealed at 250 °C for 30 min were determined to be approximately 0.51 cm^2/Vs and -12.1 V, respectively. To study the effects of the heat treatments, we measured the depth concentration profile of elements from AES surveys of $Ag/IZO/SiO_2/Si$ samples at various etching times. Inter-diffusion between the printed Ag and the IZO was observed from the AES measurements.

Acknowledgments

This study was supported by the Development of New Materials and Solution Process for LCD Backplanes funded by ISTK (B551179-09-06-00).

References

1. H. Sirringhaus, T. Kawase, R. H. Friend, T. Shimoda, M. Inbasekaran, W. Wu and E. P. Woo, Science, 290 (2002) 2123-2126.
2. S-H. Ko Park, D.-H. Cho, C.-S. Hwang, S. Yang, M. K. Ryu, C.-W. Byun, S. M. Yoon, W.-S. Cheong, K. I. Cho and J.-H. Jeon, ETRI Journal, 31 (2009) 653-659.
3. T. Kamiya, K. Nomura, M. Hirano and H. Hosino, Phys. Status Solid C, 5 (2008) 3098-3100.
4. T. Kamiya, K. Nomura and H. Hosino, Phys. Status Solid A, 206 (2009) 860-867.
5. J.-H. Shin, J.-S. Lee, C.-S. Hwang, S.-H. Ko Park, W.-S. Cheong, M. K. Ryu, C.-W. Byun, J.-I. Lee and H. Y. Chu, ETRI Journal, 31 (2009) 62-64.
6. D. H. Lee, S. Y. Han, G. S. Hermanc and C. H. Chang, J. Mater. Chem., 19 (2009) 3135-3137.
7. Y. S. Yang, I. K. You, H. Han, J. B. Koo, S. C. Lim, S. W. Jung, B. S. Na, H. M. Kim, M. Kim, and S. H. Moon, ETRI Journal, 35 (2013) 571-577.
8. Y. Shimura, K. Nomura, H. Yanagi, T. Kamiya, M. Hirano and H. Hosono, Thin Solid Films, 516 (2008) 5899-5902.
9. W. S. Choi, Electronic Materials Letters, 8 (2012) 87-90.
10. S. M. Sze, Physics of Semiconductor Devices, (Wiley, New York, 2nd ed., 1981), p. 395.
11. 11. J. Bartolome, D. Maestre, A. Cremades, M. Amatti and J. Piqueras, Acta Materialia, 61 (2013) 1932-1943.
12. M. Kim, J. B. Koo, K. J. Baeg, S. W. Jung, B. K. Ju and I. K. You, Applied Physics Letters, 101 (2012) 133306-1-133306-5.
13. H.-K. Kim, M.-S. Yi and S.-N. Lee, Thin Solid Films, 517 (2009) 4039-4042.